DOI: 10.15669/pnst.8.76

Progress in Nuclear Science and Technology
Volume 8 (2025) pp. 76-81

ARTICLE

Inherent Safety Free-Scale Reactor KAMADO-FSR Estimation of Investment and Cost

Tetsuo MATSUMURA [1*] and Takanori KAMEYAMA [2]

[1] *Department of Nuclear Engineering,* [2] *Global Research Institute of Nuclear Energy, Tokai University, 4-1-1 Kitakaname, Hiratsuka City, Kanagawa Prefecture, 259-1292, Japan*

We designed a new concept of an inherent safety and free-scale reactor, KAMADO-FSR, which uses a two-phase flow for cooling, similar to BWR (Boiling Water Reactor). The fuel assembly, consisting of a SiC block, is loaded in an atmospheric pressure reactor water pool. As the SiC block fuel assembly becomes a pressure boundary, the present reactor concept requires no pressure vessel. With the high thermal conductivity of SiC, the fuel assembly allows the coolant to become dry-out conditions, eliminating the need for steam drying equipment and improving safety performance. The power scale can be varied from 300 MWe to 1000 MWe without modularization, and the reactor's investment and cost can also be reduced significantly.

KEYWORDS: inherent safety, free scale, SiC block, two-phase flow, spectral shift, cost, investment

I. Introduction

Nuclear power plants are constantly required to improve their safety and economic efficiency. With the improvement of the existing reactors, new types of reactors with high safety and economy are also being developed, such as small modular reactors (SMR).[1)] We have proposed a new concept KAMADO with inherent safety by providing the fuel assembly with the SiC block containing UO_2 fuel pellets.[2-4)]

In the KAMADO concept, the SiC block is responsible for transmitting the fuel's fission reaction heat during reactor operation, removing the fuel's decay heat after the reactor shutdown, and ensuring inherent safety. Within the KAMADO concepts, we conducted an economic study of KAMADO-FSR (Free-Scale Reactor), in which we use two-phase flows for cooling the core without a pressure vessel and active safety protection systems, as shown in **Fig. 1(a)**.

The KAMADO-FSR can improve its reactor power scale. The power scale can be increased from 300 MWe to 1000 MWe by adding a turbine and several pieces of equipment without modularization, significantly reducing reactor investment and costs.

The high thermal conductivity of SiC allows the fuel assembly to be in the coolant dry-out conditions, eliminates steam dryer equipment, and improves safety performance.

The KAMADO concept can also be applied to replace the fuel assembly of existing LWRs[3)] and a high flux reactor.[4)]

II. Fuel assembly and Core concept

The fuel assembly, consisting of a SiC block, is loaded in an atmospheric pressure reactor water pool, and the heat generated by the fuel is transferred to a two-phase flow inside

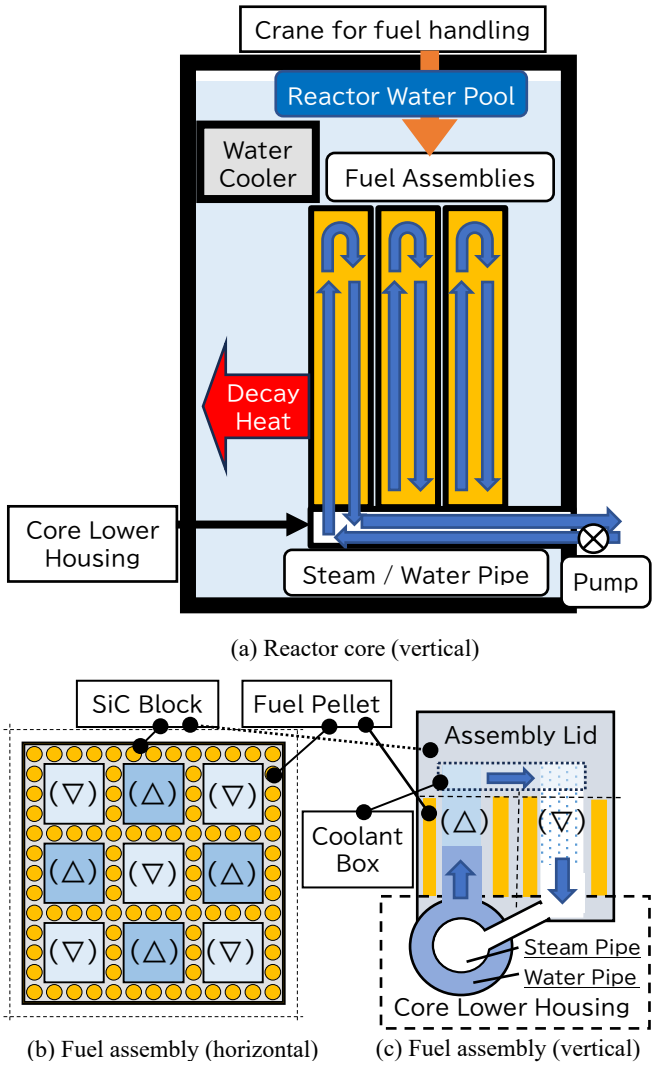

Fig. 1 Concept of KAMADO-FSR fuel assembly

*Corresponding author, E-mail: matsu@powerm.tech

the surface of the fuel assembly to the reactor water pool (final heat sink). The fuel pellets are installed in holes made in the SiC blocks (**Fig. 1(b)**). Coolant passes through each ascending flow path (△) from the water pipe in the lower core housing and is collected and mixed in a coolant box installed inside the assembly lid (**Fig. 1(c)**). While being heated and turned into steam, it passes through each descending flow path (▽) from the coolant box and reaches and collects into the steam pipe in the lower core housing. Because the fuel assembly allows the coolant to become dry-out conditions, the coolant is wholly converted into steam ($\chi = 1$) at the fuel assembly outlet, eliminating the need for steam separators and other steam drying equipment and improving safety performance.

Combining the steam and water pipes into one double pipe can simplify the structure of the core lower housing (**Fig. 1(c)**). Because the coolant mass flow is lower than that of a commercial BWR (Boiling Water Reactor) and the mixing effect of the coolant box, the pressure drop of the two-phase flow in the fuel assembly is relatively smaller than that of a BWR (about 15 kPa).

The fuel assemblies are loaded in the same way as those in commercial BWRs. They are fixed to the core lower housing with bolts. Once they are unfixed, they can be easily handled over the reactor water pool using an ordinary crane (**Fig. 1(a)**). The fuel assembly is securely fixed to the core lower housing to prevent popping out. **Table 1** shows the specifications of the fuel assembly. The average liner heat rate (LHR) is 13.2 kW/m, lower than the BWR's.

Table 1 Specifications of KAMADO-FSR fuel assembly

Item	Value
BWR & KAMADO-FSR common items	
Fuel assembly outer dimension	139.0 mm×139.0 mm
Fuel assembly pitch	152.4 mm
Fuel assembly power generation	4.31 MW
Fuel assembly height	3.7 m
Plant coolant pressure	7.02 MPa
Saturated temperature	286 ℃ (559 K)
Fuel type	^{235}U enriched UO_2
KAMADO-FSR specific items	
Fuel Pellet diameter	8.19 mm
Number of fuel stacks	88
Fuel pitch	10.54 mm
Coolant mass flow	2.55 kg/s
Inlet water temperature	250 ℃ (523 K)
Linear heat rate	13.2 kW/m
Uranium mass	149 kg

III. Numerical Analyses

1. Mechanical Analysis

KAMADO-FSR fuel assembly consists of a significant pressure difference between the inside (plant coolant pressure, 7.02 MPa) and outside (atmospheric pressure, 0.1 MPa) of the assembly, which results in the generation of tensile stress in the assembly. The tensile stress is calculated using the finite element analysis system LISA.[5] The surface of the assembly is covered with a 1-mm-thick plate of SiO_2 for heat insulation. The calculation results showed that a maximum stress of 34 MPa was generated at some central SiC blocks (**Fig. 2**). This value is smaller than the tensile strength of SiC (approximately 200 MPa), and thus, the soundness of the SiC block can be ensured.

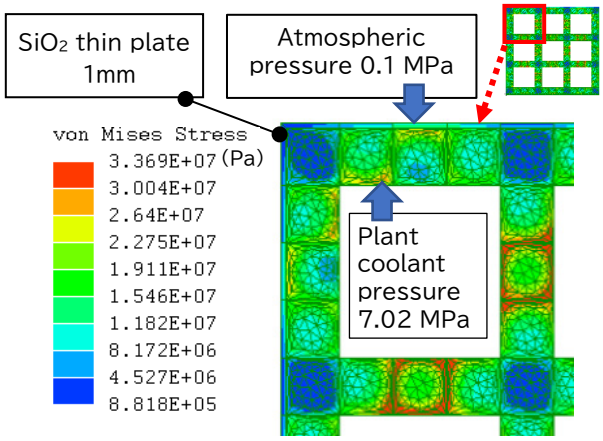

Fig. 2 Tensile stress on SiC block during operation

2. Thermal-Hydraulic Analysis

Understanding the coolant's phase change in the fuel assembly is essential. Assuming the linear heat generation rate (LHR) at the core position is constant, the core saturation position (k_s), wherein the saturated temperature is reached, can be calculated with the enthalpy at the core inlet (quality $\chi = 0$, temperature $T = 250$℃), the core outlet ($\chi = 1$, $T = 286$℃), and saturated water.

Due to a descending flow, it isn't easy to evaluate the quality where the dry out occurs (x_d). For this reason, assuming $x_d = 0.6$ from experimental data,[6] the saturation height is 0.80 m in the ascending flow path, and the dry out height is 2.64 m in the descending flow path (**Fig. 3**).

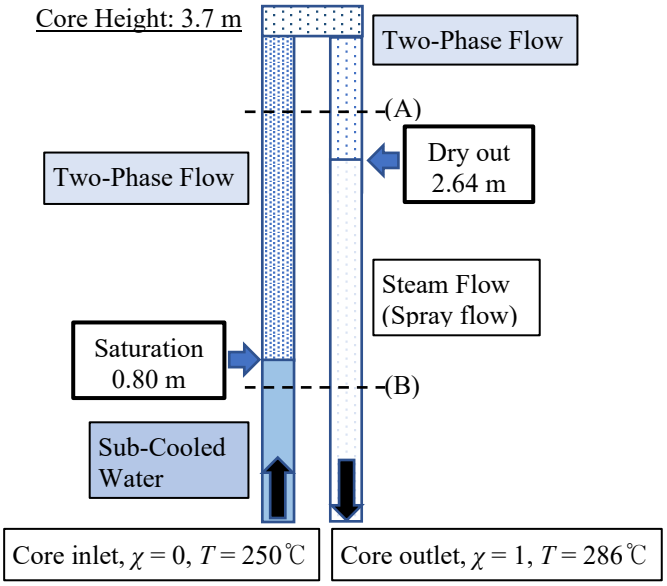

Fig. 3 Positional relationship of saturation, dry out, and others in KAMADO-FSR fuel assembly

The void ratio is critical for nuclear calculations, which is described later. Therefore, the void ratio is evaluated by a simple calculation using the slip ratio. Slip ratio S is calculated by Thom's equation, given in Eq. (1),

$$S = 0.93\left(\frac{\rho_L}{\rho_G}\right)^{0.11} + 0.07\left(\frac{\rho_L}{\rho_G}\right)^{0.561} \quad (1),$$

where ρ_L or ρ_G is density of liquid or gas (kg/m^3). Quality χ and void ratio α are calculated by Eqs. (2) and (3), respectively. W is linear heat generation rate (W/m), Δk is coolant flow path length from the saturated position (m), G is mass flow rate in the fuel assembly (kg/s), and H_c or H_{cg} is specific enthalpies of saturated water or steam (J/kg) in Eq. (2).

$$\chi = \frac{W\Delta k/G - H_c}{H_{cg} - H_c} \quad (2),$$

$$\alpha = \frac{\chi S}{1 + \chi(S-1)} \quad (3).$$

Figure 4 shows the calculated changes of χ and α with core height. The slip ratio from Eq. (1) cannot be applied to the descending flow. Therefore, in the case of a descending flow, it is assumed that $S = 1$ and the void ratio and quality are equal. The average void ratios are 55% ascending and 70% descending, respectively.

In the future, dry out, quality, and void ratio will be examined in ascending and descending flow.

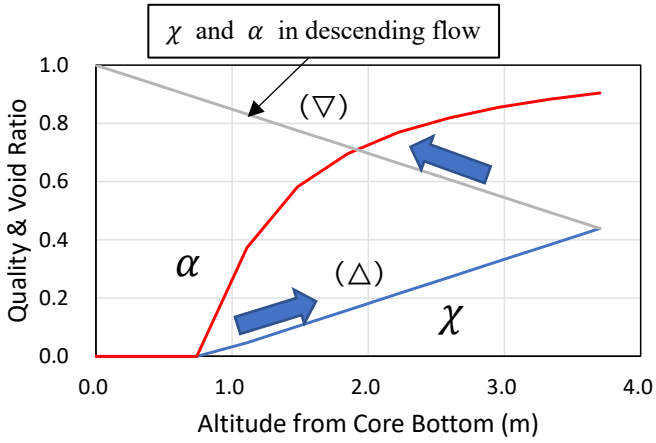

Fig. 4 Changes of quality χ and void ratio α with altitude from core bottom

3. Fuel Temperature Analysis

Calculating the fuel temperature distribution requires the thermal conductivities of UO_2, SiC, and SiO_2, as well as the heat transfer coefficient from the SiC block to the coolant. As shown in **Fig. 5**, the temperature calculations for the cross sections (A) and (B) in **Fig. 3** were performed with LISA.

In section (A), the ascending and descending flows are two-phase. The heat transfer coefficient (h) from the SiC block to the two-phase flow is 138 kW/m^2/K, which was calculated using the following Jens-Lottes equation[7] by Eq. (4).

$$h = \frac{1}{0.79} q_w^{3/4} \exp\left(\frac{p}{6.2 \times 10^6}\right) \quad (4),$$

where q_w is heat flux (W/m^2), and p is pressure (Pa).

In section (B), the ascending flow occurs in subcooled water, and the descending flow occurs after the dry-out. After the dry out, the coolant flow becomes a spray flow, and the heat transfer performance is significantly reduced. Since the heat transfer of the spray flow is complicated, the heat transfer coefficient of steam is conservatively applied here for the spray flow.

The cooling performance coefficients of the subcooled water and steam, evaluated by the Dittus-Boelter formula in Eq. (5), and heat transfer coefficient h are 12.8 and 5.42 kW/m^2/K, respectively, where λ is thermal conductivity (W/m/K) and D is equivalent diameter of the coolant flow path (m).

$$h = 0.023\, Re^{0.8}\, Pr^{0.4} \frac{\lambda}{D} \quad (5).$$

Fuel assemblies are located in the reactor water pool (atmospheric pressure). Fuel heat also flows to the reactor water pool. Vapor voids are generated locally on the surface of the fuel assembly. The heat transfer coefficient to the reactor water pool is calculated in Eq. (5), assuming that the flow velocity of water is 0.1 m/s. The heat transfer coefficient to the reactor water pool is 1.06 kW/m^2/K.

In cross sections (A) and (B), the maximum fuel temperatures are 1034 and 1209 K, respectively (**Fig. 5(a), (b)**). These temperatures are sufficiently low for fuel integrity and reactor core safety.

The 1 mm-thick SiO_2 heat-insulating material suppresses heat transfer to the reactor water pool. However, approximately 10% of the fuel assembly, with a power of 4.31 MW, such as 393 kW, flows out. This heat loss can be reduced by changing the insulating material or increasing its thickness.

During an event such as LOCA or LOF, the coolant cannot be expected to deliver cooling performance. **Figure 5(c)** shows the results of fuel temperature distribution with the cooling performance of the reactor water pool only, assuming the decay heat is conservatively 10% of the fuel assembly power during normal operation. In this case, the maximum temperature is 942 K, which can sufficiently ensure fuel safety.

These temperature calculations do not consider the gap heat transfer between the fuel pellet and the SiC block. A temperature difference (gap) of approximately 100 K is noted in the BWR. As the average LHR (13.2 kW/m) of the KAMADO-FSR is smaller than that of the BWR (approximately 19 kW/m), the temperature gap is expected to be smaller than that of the BWR. Even if the temperature at the center of the fuel pellet is likely to rise by approximately 100 K, the impact on fuel integrity is small. In addition, the temperature gap can be reduced if helium gas of roughly 1 MPa pressure is filled into the fuel pellet holes during fuel assembly manufacturing, as in the case of the BWR.[8]

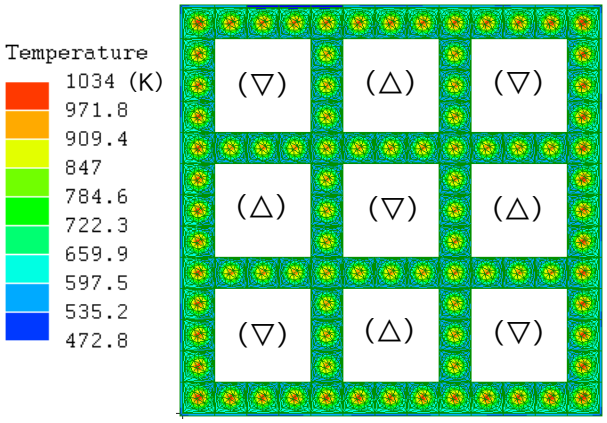

(a) Section (A) in operation

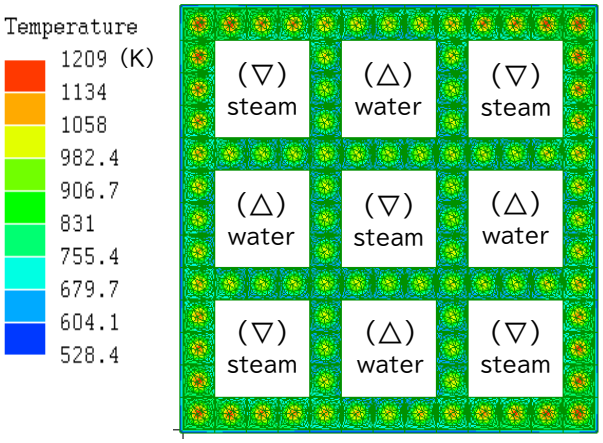

(b) Section (B) in operation

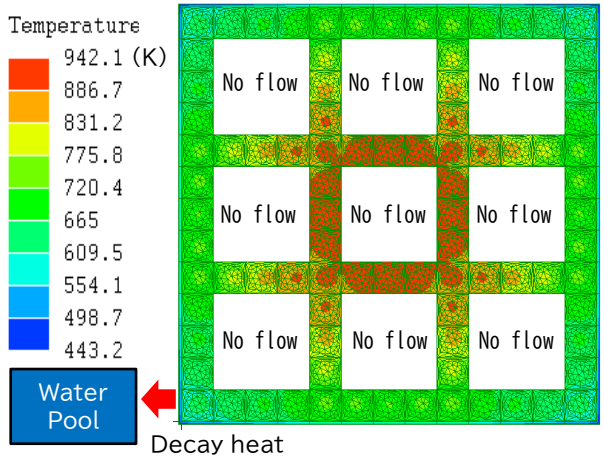

(c) Section (B) at LOCA / LOF

Fig. 5 Temperature distributions in KAMADO-FSR fuel assembly

4. Neutronic Analysis

The Monte Carlo Codes MVP[9] and MVP-BURN[10] with their libraries based on JENDL-4.0, were used in the neutronic calculations. The initial nuclide composition was based on the BWR Step-III values[11]. **Figure 6** shows the burnup dependence of k_∞ for these fuel assemblies. In the KAMADO-FSR burnup calculation, the average void ratios of 55% and 70% were applied in the ascending and descending flow, respectively (Fig. 4). The void condition was 40% in the BWR 9 × 9 burnup calculation.

The nuclear reaction characteristics of the KAMADO-FSR fuel assembly are almost the same as those of the BWR fuel assembly without Gd-doped fuels. In this core, neutron spectral shift operation is also possible by inserting water exclusion SiC plates outside the fuel assembly (**Fig. 7**), which are set to fully insert at the beginning of cycle (BOC) and entirely withdraw at the end of cycle (EOC). The insertion length is the effective fuel assembly height of 3.7m. The water exclusion SiC plates can increase the core average k_∞ of 5 batches at the end of the reactor operation cycle by 5% $\Delta k/k$ from 1.0398 to 1.0938. The KAMADO-FSR core can reduce fuel enrichment and Gd-doped fuel pellets. The conversion rate of KAMDO-FSR is 0.57, while it increases to 0.69 with spectral shift.

As the void fraction of the two-phase flow in the center of the fuel is high (55% and 70%), the effect of water exclusion by SiC plates is excellent. The control and safety plates, filled with B_4C, are also inserted around the fuel assemblies like the water exclusion SiC plates, but in small numbers. It is considered that the drive mechanism for the SiC plate and the control/safety plates will be installed on top of the fuel assembly.

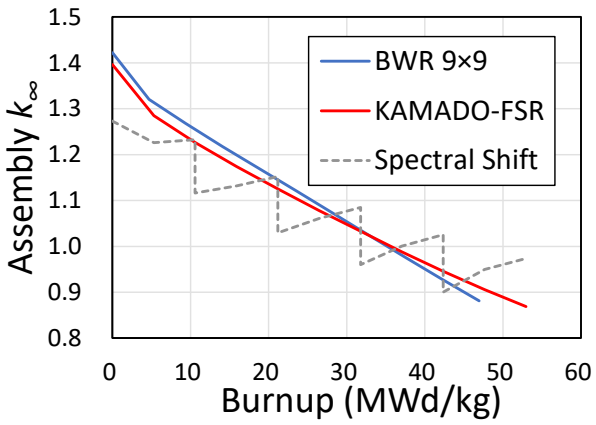

Fig. 6 Changes of fuel assembly k_∞ with burnup

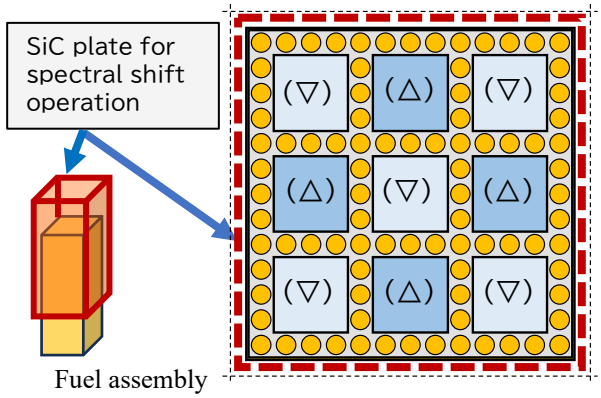

Fig. 7 Layouts of water exclusion SiC plate

IV. Power Scale-Up and Economic Analyses

KAMADO-FSR (free scale reactor) operates as a small nuclear power plant of 300 MW at first and can be easily extended to 1000 MW without modulization. Suppose a 40 ×

40 fuel assembly space (approximately 6 m × 6 m) is prepared (**Fig. 8**). In that case, the fuel assemblies are installed in the region (A) at first (300 MW), and the additional fuel assemblies are loaded in the region (B) at the next step (1000 MW). **Table 2** shows capital costs (%) for nuclear power plants of 650 MWe BWR and scaling factor (n) in Cost(P_1) = Cost(P_0)×(P_1/ P_0)^n.[12] The cost of "Reactor plant equipment" is estimated to be 1/10 because there is no pressure vessel, recirculation pumps, or active safety equipment. The SiC block fuel assembly is included in fuel costs but not construction costs. From this capital cost and the scaling law, the construction cost of 300 MWe KAMADO-FSR is estimated to be 61% of the 650 MWe BWR. On the opportunity for scaling up the KAMADO-FSR to 1000 MWe, the turbine, electrical, and heat rejection plant systems have to be extended; accordingly, the construction cost increases to 95% of that for the 650 MWe BWR. The power generation cost related to the construction cost divided by power (kWe) is about 62%, compared with the 650 MWe BWR.

KAMADO-FSR offers the following benefits for investment:

- The 300 MWe KAMADO-FSR construction cost is lower.
- Shorter construction time allows faster return.
- Scalability reassures stakeholders about its adaptability to future energy demands.
- As 300 MWe KAMADO-FSR offers potential returns, scaling up means expecting more significant returns while keeping a lower investment.

Table 2 Capital costs of nuclear power plants

Item	650MWe BWR (%)	Scaling factor (n)	300MWe KAMADO -FSR (%)
Direct costs			
Land and land rights	0.1	0.2	0.1
Reactor plant equipment	27.6	0.3	2.2*
Turbine plant equipment	14.7	0.75	8.2
Electrical plant equipment	13.2	0.37	9.9
Heat rejection equipment	2.2	0.4	1.6
Miscellaneous equipment	15.2	0.2	13.0
Construction	10.1	0.2	8.7
Direct costs total	**83.1**		**43.7**
Indirect costs total	**11.3**		**11.3**
Other costs total	**5.6**		**5.6**
Total	**100**		**60.6**

*: reduced to 1/10 by eliminating pressure vessel, recirculation pumps or active safety equipment.

V. Discussion

1. SiC Materials

SiC materials are known to have high strength but are fragile. For this reason, SiC/SiC composite materials in SiC fibers have been explored.[13] Various methods are used to manufacture SiC parts/blocks, such as atmospheric pressure sintering, hot press, hot isotropic press, chemical vapor deposition, reaction sintering, and chemical vapor infiltration. As the mechanical performance of SiC differs depending on these methods, it is necessary to focus on the research and development of SiC manufacturing methods.

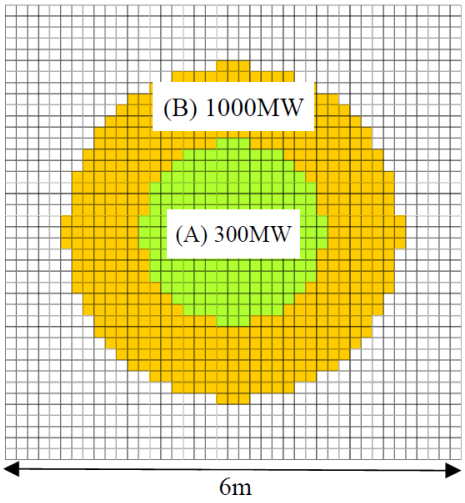

Fig. 8 Concept of reactor power scale-up

Since SiC is hard to weld directly, a method for sealing the SiC block after filling it with fuel pellets must be devised. Because of the large structure of the SiC block, mechanical methods such as bolting are considered instead of brazing. Although corrosion of SiC is also being discussed, countermeasures are being considered. [14,15]

It has been reported that the thermal conductivity of SiC deteriorates as irradiation damages accumulate.[16] We analyzed the temperature distribution when the thermal conductivity of SiC was reduced to 100 W/m/K, which is half of that in the as-fabricated fresh conditions. Compared to the result at LOCA/LOF in the previous temperature analysis shown in Fig. 5(c), the maximum fuel temperatures (1180 K) increased by 238 K because the heat transfer distance of SiC is long. But the fuel temperatures were acceptable. During operation, the temperature rise is kept below 40K because the heat transfer distance of SiC is short. It has also been reported that the heat conductivity deterioration with irradiation depends on the method of manufacturing SiC or fabricating SiC/SiC composite materials.[17]

Since SiC has high thermal conductivity (at least 100 W/m/K) and low thermal expansion coefficient (4.0 × 10^{-6}/°C), the effects of temperature gradient and the thermal stress in SiC are considered minor.

2. Safety and Others

- During LOCA and LOF, the moderator temperature coefficient is kept negative, the power is reduced, and the reactor water pool directly cools the decay heat to ensure the integrity of the fuel assemblies. Regarding TOP (transient over power), such as a control rod withdrawal accident, the power coefficient is also kept negative, and the power is expected to decrease after the temporary peaking. Accordingly, the impact on fuel integrity is expected to be small.

- The core is made of high-melting-point ceramic SiC and contains no metal materials, making accident-tolerant fuel (ATF) possible and preventing core meltdown.
- If the amount of water in the reactor water pool decreases, it may damage the fuel assemblies. Safety measures like emergency water tanks should also be installed to replenish the reactor water pool.
- The core is underwater, and the fluid seismic isolation system is in place and highly earthquake-resistant.
- Although KAMADO-FSR does not have a recirculation pump like BWR, the power output can be fine-tuned by adjusting the inlet water temperature.

VI. Conclusion

We designed the basic concept of KAMADO-FSR and confirmed its feasibility by numerical analyses. The SiC block of the fuel assembly is utilized to withstand the pressure difference between plant coolant pressure (7.02 MPa) and the reactor water pool (0.1 MPa), which requires no pressure vessel for KAMADO-FSR. In LOCA or LOF cases, the decay heat is dissipated directly from the fuel assembly surface to the reactor water pool (final heat sink). No active safety systems are required to cool the fuel during the accidents, which provides inherent safety. Also, the spectral shift operation of KAMADO-FSR can reduce the fuel ^{235}U enrichment and Gd-doped fuel pellets. KAMADO-FSR operates as a small nuclear power plant of 300 MWe at first and can be easily extended to 1000 MWe without additional modulization. The construction cost of 300 MWe KAMADO-FSR is estimated to be 61% of the 650 MWe BWR, and the power generation cost is about 62% after extending to 1000 MWe.

The KAMADO-FSR concept can be one of the candidates for the next-generation thermal reactor because the reactor is inherently safe, economical, and small without a pressure vessel.

Main challenges remain, such as fuel assembly manufacturing methods, irradiation effects on SiC material properties, and detailed thermal-hydraulic behavior. We plan to proceed with the detailed design of the fuel assembly and reactor plant in the future.

References

1) Small Modular Reactor: Advances in SMR Develop 2024, IAEA (2024). https://www-pub.iaea.org/MTCD/Publications/PDF/p15790-PUB9062_web.pdf
2) T. Matsumura, T. Kameyama, "Basic Concept of Inherent Safety Free-Scale Reactor "KAMADO-FSR," NTHAS12, Miyazaki, Japan, Oct. 30 – Nov. 2, N12P1121 (2022).
3) T. Matsumura, T. Kameyama, "New Concept of Accident Tolerant Fuel Assembly Composed of SiC Block for KAMADO-BWR," *Proc. Schl. Eng. Tokai Univ*., Ser. E 47, 7-13, DOI: 10.18995/24343641.47.7 (2022).
4) T. Matsumura, T. Kameyama, "Design Concept of a High Flux Reactor "KAMADO-HFR" adjusting to ^{99}Mo Production for Medical Diagnostics," *Proc. Schl. Eng. Tokai Uni*v., **64**[1], 7-12(2024), DOI: 10.18995/24343633. 64-1.7.
5) LISA Finite Element Analysis, Sonnenhof Holdings, https://www.lisafea.com/index.html
6) JSME Heat Transfer Handbook, JSME (1993).
7) W. H. Jens, P. A. Lottes; "Analysis of Heat Transfer, Pressure Drop and Density Date for High Pressure Water," ANL-4627 (1951).
8) J. Yamashita, S. Saito, "BWR Core with High Burn-up and High Uranium Utilization," *The Hitachi-hyoron*, **68**[4], (1986) [in Japanese].
9) Y. Nagaya, K. Okumura, T. Sakurai, T. Mori, "MVP/GMVP Version 3: General Purpose Monte Carlo Codes for Neutron and Photon Transport Calculations Based on Continuous Energy and Multigroup Methods," JAEA-Data/Code 2016-019 (2016).
10) K. Okumura, T. Mori, M. Nakagawa, K. Kaneko, "Validation of a Continuous-energy Monte Carlo Burn-up Code MVP-BURN and Its Application to Analysis of Post Irradiation Experiment," *J. Nucl. Sci. Technol*., **37**, 128 (2000).
11) K. Okumura, K. Sugino, K. Kojima, T. Jin, T Okamoto, J. Katakura, "A Set of ORIGEN2 Cross Section Libraries Based on JENDL-4.0: ORLIBJ40," JAEA-Data/Code2012-032 (2013).
12) Reduction of Capital Costs of Nuclear Power Plants, OECD/NEA-2088 (2000).
13) K. Walter, "Carbon Fiber Reinforced Silicon Carbide Composites (C/SiC, C/C-SiC)," *Handbook of Ceramic Composites*, Springer, Boston, MA (2005).
14) A. Tsuchiya, J. Matsunaga, K. Sakamoto, M. Sasaki, H. Miyata, R. Ishibashi, "Development of FeCrAl-ODS steels and SiC/SiC composite for BWR fuel claddings," *Journal of AESJ*, **66**[.9] 453-457 (2024) [in Japanese].
15) M. Owaki, T. Nishimura, "Development of SiC cladding," *Journal of AESJ*, **66**[9], 458-462 (2024), [in Japanese].
16) A. Hasegawa, "Neutron Irradiation Effects of SiC and SiC/SiC Composite," *Journal of Plasma and Fusion Research*, **80**[1], 24-30 (2004), [in Japanese].
17) Y. Katoh. "Status and Prospects of SiC-Based Ceramic Composites for Fusion and Advanced Fission Applications," *Journal of Plasma and Fusion Research*, **80**[1], 18-23 (2004), [in Japanese].